

The effect of the noise on the dynamics of soliton generation in microresonator

Hawraa A. Mezban¹, H. A. Sultan²

¹*Department of Physics, College of Education for Pure Sciences, University of Basrah, Basrah, Iraq*

²*Department of Physics, College of Education for Pure Sciences, University of Basrah, Basrah, Iraq*

*Corresponding author: hawraalhasen@gmail.com

Received 12 Feb, 2024, Accepted 22 Apr. 2024, published 1 Jun 2024.

DOI: 10.52113/2/11.01.2024/48-61

Abstract: The study demonstrated that noise changes the number of modes that can oscillate within the small cavity, and the spectral power is concentrated around the fundamental frequency. We also observed a reduction in the distortion that arises from the dispersive solitaire. This behaviour can be attributed to the magnitude of the pulse strength or the loss of its frequency due to the arbitrary interaction between the pulse train and the linear and nonlinear refractive index of the microcavity. The relationship between the dispersion and nonlinearity phenomena inside the microresonators is major in determining the inside field dynamics. The study showed that as the noise in microresonators cannot be cancelled, it is recommended to use a proper pulse width, intensity distribution, and power.

Keywords: frequency comb, noise, Lugiato–Lefever equation, Dissipative Kerr solitons, nonlinear optics.

1. Introduction

Microcavity, also known as a microresonator (MR), is a structure that is made by either bending a waveguide into a ring shape or adding reflecting surfaces on both sides of an optical medium or spacer layer. Whereas the latter is called a moving wave cavity, the former is called a stationary wave cavity. Its thickness is usually a few micrometers, sometimes even reaching the nanoscale for the spacer layer, for this reason, the term "microcavity" is employed. As with regular lasers, this setup creates an optical cavity or optical resonator that allows standing waves to develop in the spacer layer or

traveling waves to circulate the ring. They can range in size from the width of hair to a few millimeters in diameter. Light is trapped in the microresonators in a way that forces it to travel around the resonator's circumference. If the resonators are of sufficiently high quality (quality factors 10^6 to 10^{10}), it is possible to store a lot of light within. Nonlinear interactions between the light and the microresonator occur at high enough intensity. This process, known as "four-wave mixing," which may turn a single hue of light into a comb with several colors [1]. It has been discovered that cascaded four-wave mixing (CFWM), processes cause frequency

combs to form in nonlinear microresonators [2]. The frequency comb's line spacing and the round-trip duration of inverted light in the micro-resonator is referred to as the FSR and, depending on the microresonator's free spectral range, can be in the gigahertz or terahertz range. Significant research interest has been shown in the optical frequency combs produced in monolithic high-quality factor microresonators [3,4]. Recently, it has been shown that dissipative Kerr solitons found in microresonators can be used to create low-noise and broad-frequency combs [5,6]. A soliton is a locally concentrated, self-reinforcing wave packet that keeps its amplitude and form while moving across a medium. In many different physical systems, including optics, fluid dynamics, and nonlinear systems, this kind of solitary wave can appear.

In the context of optics, solitons are most commonly observed in optical fibers [7,8]. The capacity of optical solitons to retain their form and speed across extended distances without attenuation or dispersion is what distinguishes them. In the fiber, the nonlinear and dispersive effects are balanced to provide this special characteristic. Owing to its intrinsic stability and harmony with the resonator's structure, the TEM₀₀ Gaussian mode is frequently the mode of choice for soliton creation in microresonators.

As a result, the stability, effective coupling, and geometry compatibility of the TEM₀₀ Gaussian mode make it a good choice for soliton production in microresonators. Achieving steady and durable soliton production in these systems requires the interaction of the TEM₀₀ Gaussian mode with the nonlinear response of the microresonator. and the production of optical frequency combs was examined [9]. The last ten years have seen the discovery of rich nonlinear dynamics in microresonators, which include solitons for breathing [10], soliton crystals [11], Stokes solitons [12], Pockels solitons [13], laser cavity solitons [14], and dark solitons [15]. In terms of applications, soliton microcombs have already been successfully used for optical frequency synthesizers [16], astronomy [17], and optical coherent communications [18]. Almost all physical systems have some noise level, and depending on the type of laser being used, this noise may take many forms. Only phase/frequency and amplitude noise that is inherent to the laser itself occurs in single-frequency [19] lasers. However, in a system that lasers at many modes at once, there is also mode-beating noise and mode-partition noise, which stand in for intermodal interference and random power transfer across modes, respectively. In the case of pulsed cavities, additional noise sources come into play. Timing jitter is one such source, which is the phase

difference between the carrier wave and the pulse envelope. Timing jitter can arise from various factors, including noise in the laser source, imperfections in the pulse generation mechanism, or external perturbations affecting the cavity [20].

There are various sources of noise [21, 22], but generally, we can say that almost all lasers share at least two of these sources. Quantum noise is the incoherent spontaneous emission in the gain medium (which frequently establishes the lower bound for system performance), and technical noise is the extra noise that is generated by the surrounding environment, such as the control electronics, vibrations, temperature changes, etc. The repetition rate of the pulsed source can also contribute to noise. Any fluctuations or variations in the repetition rate can introduce timing errors or inconsistencies between consecutive pulses, leading to temporal noise in the output. Understanding and characterising these different types of noise is crucial in the design and operation of cavity-based systems, as they can significantly impact the performance and stability of various applications such as lasers, frequency combs, and optical communication systems.

In this work, the primary objective is to investigate and analyze the influence of noise. We approached this study from a theoretical standpoint by introducing additional terms or

noise sources into the analysis. One specific noise source that was incorporated into the microresonator field is known as White Gaussian Noise (WGN). A random signal with a flat power spectral density, or one that has equal strength at every frequency, is called white Gaussian noise (WGN). Our goal is to mimic and account for several sources of noise that might impact the system's performance by introducing WGN into the microresonator field.

2. Theory

We begin our analysis of the dynamics of the soliton formation with a numerical simulation based on the Lugiato-Lefever equation (LLE) [23], such as noise effects. In simulations of soliton number management by back tuning of the laser after production and the stability of a multi-soliton state, noise effects have been considered [24]. This model is used to examine the dynamics of direct soliton formation. Noise effects will cause an extra pump phase detuning in the LLE in simulations, and we represent the generalized LLE [25]

$$E^{m+1}(0, \tau) = \sqrt{\theta}E_0 + \sqrt{1 - \theta}E^{(m)}(L, \tau)e^{i\varphi_0} \quad (1)$$

Therefore, $E^{m+1}(0, \tau)$ is the intracavity field at the beginning of the $(m + 1)^{\text{th}}$ roundtrip, and L is the cavity length for the SiN microring resonator after the m^{th} roundtrip. φ_0 provides the intracavity field's linear phase accumulation for

the pump field during a single roundtrip, while θ indicates the coupler's transmission coefficient. It might be argued that the intracavity field envelope varies little between consecutive round trips in the limit of minimal loss. In these circumstances, the prior infinite-dimensional map can be averaged to produce the externally driven NLSE. [26]

$$t_r \frac{\partial E(t,\tau)}{\partial t} = [-(\alpha + i\delta_o) + iL \sum_{k \geq 2} \frac{\beta_k}{k!} \left(i \frac{\partial}{\partial \tau}\right)^k + iL\gamma |E(t,\tau)|^2]E(t,\tau) + \sqrt{\theta}E_{in} \quad (2)$$

$E(t,\tau)$ denotes the intracavity field, the ordinary (fast) time variable τ is responsible for characterizing the temporal profile of the field, while the slow time-scale t governs the evolution of this profile over multiple round trips, the roundtrip duration is ($t_r = 2Ln_0/C$) [27], Additionally, it is presumed that the field will follow the cavity roundtrip time, which is

$$E(t + 2, \tau) = E(t, \tau) \quad (3)$$

which determines the field's temporal profile in ordinary (fast) time [28]. The definitions of the other variables in the equation are as follows: β is the second-order dispersion coefficient, $\alpha = (\alpha_i + \theta)/2$ describes the total cavity losses. The quantity $\delta_0 = 2k\pi - \varphi_0 \ll 1$ is the order of the cavity resonance closest to the driving field being detuned by the cavity from the nearest resonance. The coefficient of power

transmission, represented by k , is associated with the dispersion coefficients β_k and γ is the nonlinear interaction coefficient. Using the nonlinear Schrodinger equation (NLSE), the LLE is a periodic boundary condition applied to a damped, driven Kerr nonlinear resonator [29]. Significantly, a slow-varying time envelope is provided, which produces a mean-field solution that does not change in the field throughout a round trip. This limitation sets the LLE apart from the more general Ikeda map [30] and provides great physical representation for a wide range of systems while making computations simpler. Particularly, simulations built on the LLE formalism have made it possible to describe the production of microcombs in a way that quantitatively correlates with reported experimental results [26].

3. Results and Discussion

The split-step Fourier method (SSFM) was used to imitate the soliton dynamics within the LLE numerically [29]. We utilize Eq. (2) to examine the dynamics associated with the direct formation of solitons. The presence of noise effects introduces an additional pump phase detuning to the LLE during the simulations. In the framework of Eq. (2), MATLAB was used to solve the numerical simulation of the soliton dynamics. The simulation parameters used in this work are displayed in Table (1) to examine intensity noise.

Table 1: The simulation parameters used in this work are the typical parameters for Fused silica [26, 31, 34]

Symbol	Description	Value	Unit
λ_0	Lasing Wavelength	1.55	μm
n_2	The nonlinear refractive index	2.4×10^{-19}	m^2/W
ω_0	the frequency of the optical cw pump	193.5	THz
n_0	the refractive index	1.99	
A_{eff}	the effective model area of the resonator mode	2.5×10^{-12}	m^2
Q	Quality factor	1.5×10^6	
θ	the external coupling coefficient	0.03	
P_{in}	input cw pump power	0.5, 1, 1.5, 2	Watt
γ	nonlinearity coefficient	1.2	$\text{W}^{-1}\text{m}^{-1}$
a	total cavity losses inside the resonator	0.00161	
β_2	dispersion coefficient	-4.7×10^{-26}	s^2m^{-1}
L	Cavity length	428.6	μm
t_R	the roundtrip time	14.28	ns
a	radius	100	μm
τ	Fast time	2	ps

3.1. The effect of the noise and fluctuations on the power distribution over the resonator modes

When noise is theoretically added, the distribution of the microresonator's output in the frequency range expands wider, especially at low values of spectral power, and the modes that are allowed to oscillate at a frequency farther from the center one also increase. While the shape of the output pulse is almost constant in the Gaussian shape without the presence of noise. Figure (1) shows that after adding noise, the output pulse (blue color) began to suffer distortion and drift towards frequencies lower

than the central frequency (dispersive waves). meaning that as the power increased, the effect of the noise on the results increased, and then the pulse shape began to saturate and stabilize in an almost constant form. Starting from power (2W) and above. The comparison with Figure (2), which represents the output of the resonator before adding noise, allows for a visual comparison of the effects of noise on the pulse shape and spectrum. Without noise, the output pulse retains a Gaussian shape and does not suffer from the same level of distortion and deviation observed in the presence of noise.

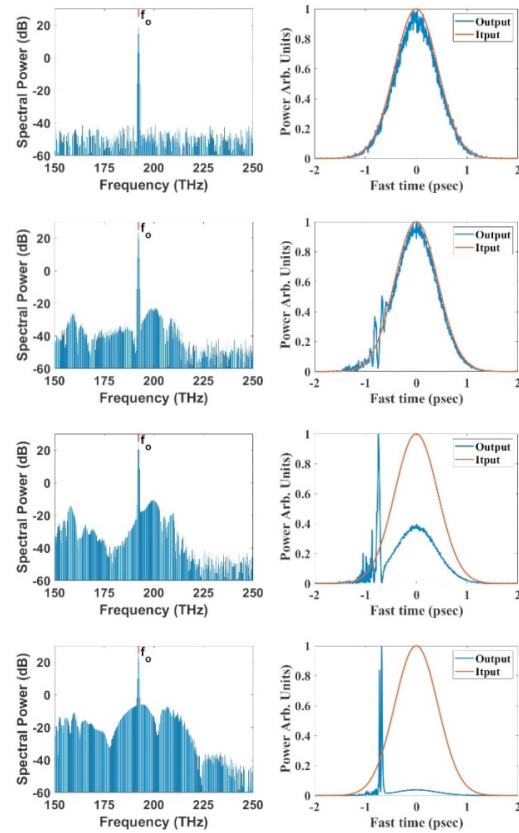


Fig. (1): (left) OFC generated, (right) input-output pulse relation with noise, for input power (1, 1.5, 1.7, and 2) respectively.

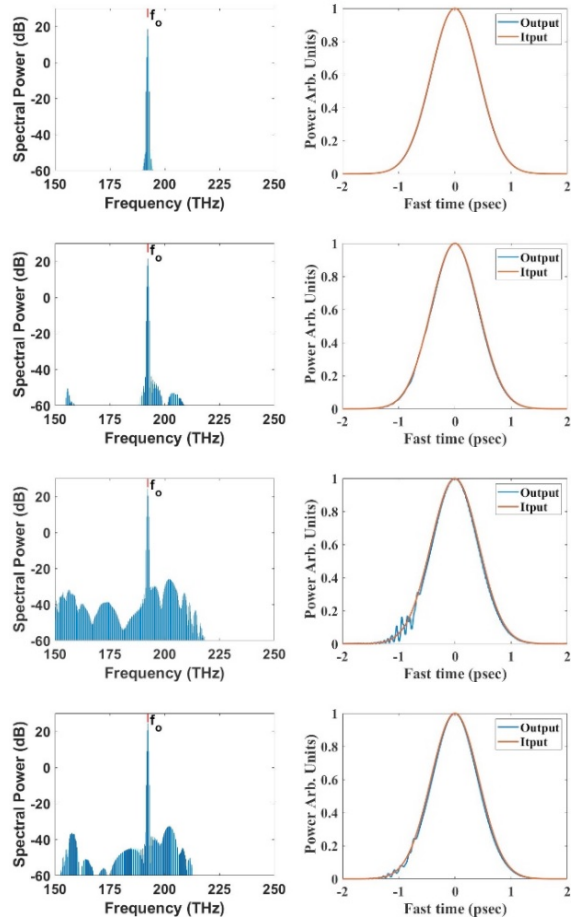


Fig. (2): (left) OFC generated, (right) input-output pulse relation without noise, for input power (1, 1.5, 1.7, and 2) respectively.

3.2. The effect of the noise and the number of round trips within the resonator

We note from Figure (3) that as the number of round trips inside the resonator increases, the presence of noise becomes more noticeable and influential. Since they indicate random or unwanted fluctuations in the signal, they have a

greater impact on the system because they accumulate over multiple round trips. The introduction of noise causes the output pulse, represented by the blue color, to undergo distortion and deviate from its original shape. This deviation is towards frequencies lower than the pulse's center frequency. The phenomenon of the pulse deviating towards lower frequencies is characterized by dispersed waves. This suggests that the noise affects the pulse in a way that spreads its energy across a wider range of frequencies. The effect of noise on the pulse becomes more pronounced as the number of round trips (slow time) increases. This implies that over time, the cumulative impact of noise on the pulse becomes more significant. As the slow time exceeds (100 ns) or above, the pulse shape reaches a state of saturation. This means that the pulse stabilizes and remains almost constant despite further increases in the number of round trips. It is clear that the noise reduces the number of modes that can oscillate inside the microcavity, the spectral power is centered at the essential frequency, and the distortion that arises from the dispersive soliton is also decreased. This behaviour can be attributed to the amount of the pulses' power, or their frequency was lost by the arbitrary interaction between the train of pulses and the microcavity linear and nonlinear refractive index.

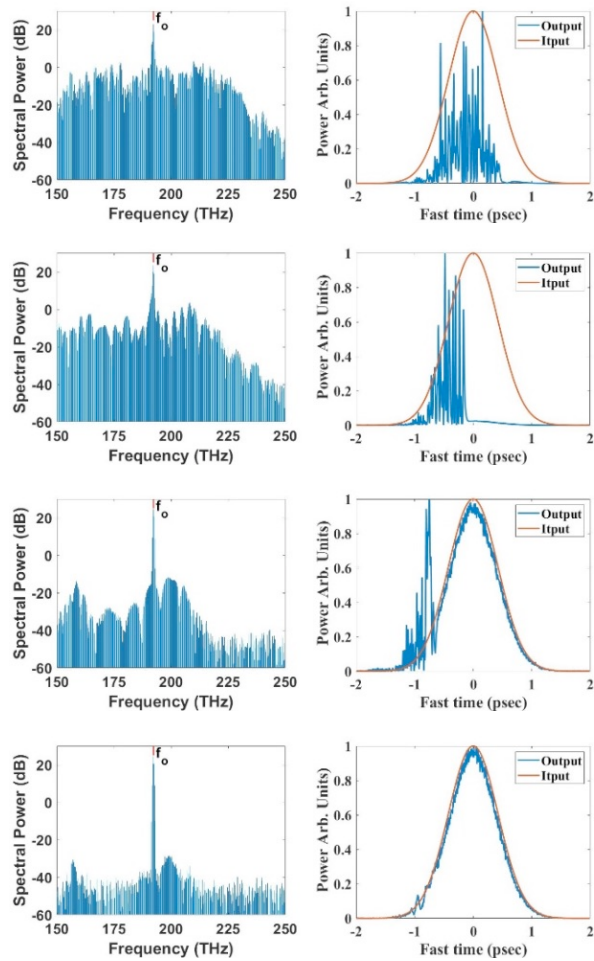


Fig. (3): (left) OFC generated, input-output pulse relation (right) with noise, for input power is (2W) and slow time value is (10, 50, 80, 100) ns respectively.

Figure (4) illustrates how the center frequency predominates when the slow time is short, how new modes start to emerge at the expense of existing modes as the number of round trips within the microresonator increases, and how dispersion causes the pulse to become wider and shorter in height over time. The previously presented Figures clearly show dispersion.

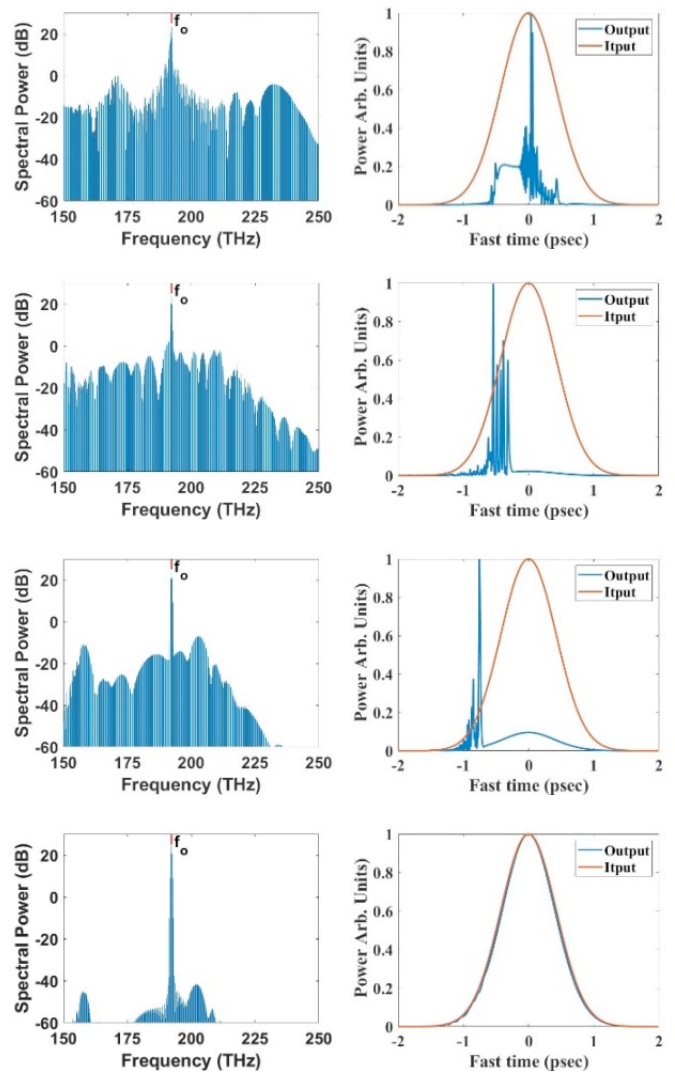


Fig. (4): (left) OFC generated, input-output pulse relation (right) without noise, for input power is (2W) and slow time value is (10, 50, 80, 100) ns respectively.

We also noticed that dispersion pulls the pulse in a certain direction (dispersive pulse).

We obtain a stable pulse that can propagate over extended distances with dispersed spectral density and little distortion as time goes on and the number of roundtrips increases. This is achieved by the system reaching a single state.

3.3. The effect of the noise, the chirp, Gaussian, and super-Gaussian on the output of the microresonator

In optical transmission systems, chirped solitons find practical applications. Ultrashort pulses, consisting of very brief bursts of light, are used to transmit information over optical fibers. However, these pulses can experience dispersion, which causes the different frequency components of the pulse to spread out over time. This dispersion can degrade the quality of the transmitted signal. Chirps in ultrashort pulses can either be positive or negative. A positive chirp means that the higher-frequency components arrive before the lower-frequency components, while a negative chirp indicates the opposite. The presence of chirp alters the pulse's temporal profile, affecting its propagation characteristics through the transmission medium. By manipulating the chirp of the ultrashort pulses, it is possible to mitigate the dispersion effects and enhance the quality and reach of optical communication systems.

The frequency chirp in the pulse has a significant influence on its optical characteristics. In the anomalous dispersion regime, which is the operating regime of the resonator, there exist simple relationships between various pulse parameters such as energy (E), pulse duration (T), and peak power (P₀), as well as oscillator parameters including

the net group delay dispersion coefficient (β) and the self-phase modulation coefficient (γ).

To prevent pulse instability, peak power P₀ must be maintained below a threshold value of P_{th}. This means that to scale energy, a pulse must be stretched, and this can only be achieved by a significant dispersion increase [35].

$$E = 2\sqrt{|\beta|P_{th}/\gamma} \quad (4)$$

In our investigation, we focus on using a particular type of resonator known as a second-order dispersion-controlled Kerr resonator for the same parameters as in Table (1). This resonator can exhibit abnormal dispersion, meaning it can cause the pulse to spread out over time. To control the chirping effect, we introduce a parameter called C. This parameter allows us to manipulate the linear frequency chirp applied to the pulse. By adjusting the value of parameter C, we can influence the extent of chirping in the pulse. We analyze the effect of the initial chirp on the Gaussian pulse during its propagation in a microresonator at a wavelength of 1550 nm. The chirped Gaussian pulse, which we use to begin this topic, is provided by [29]

$$U(0, T) = U_0 \exp\left(-\frac{(1+iC)}{2} \frac{T^2}{T_0^2}\right) \quad (5)$$

The pulse envelope's internal frequency change is described by the chirp parameter C. The Lugiato-Lefever equation has to be solved to provide a comprehensive description of all

influences that impact the propagating signal. The studies of femtosecond pulse propagation such as in [36] served as the foundation for our simulation.

As shown in Figure (5), this equation reduces to an unchirped Gaussian pulse, represented by Eq. (6), if $C = 0$.

$$U(0, T) = U_0 \exp\left(-\frac{T^2}{2T_0^2}\right) \quad (6)$$

This is because anomalous dispersion regimes combine the effects of loss, dispersion, and nonlinearity to produce an initially un-chirped Gaussian pulse ($C = 0$), This represents the TEM_{00} of the Gaussian beam.

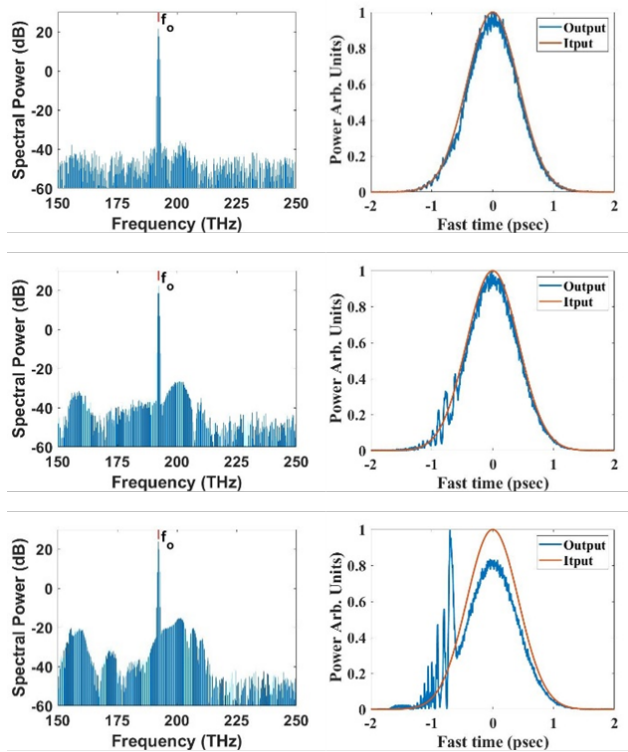


Fig. (5): (left) OFC generated, (right) input-output pulse relation with noise and without chirp ($C=0$), for input power, is (1, 1.2, 1.7) W respectively

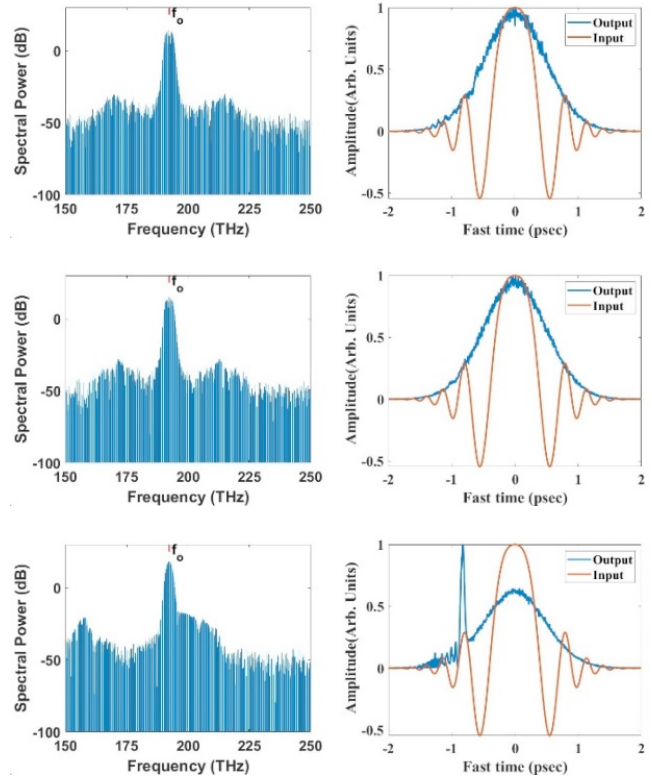


Fig. (6): (left) OFC generated, input-output pulse relation (right) with noise and chirp effects together, for input power is (1, 1.2, 1.7) W respectively.

When looking at Figure (6), we can examine how the left optical frequency comb (OFC) with combined noise and chirp effects, as well as different input power levels, creates the input-output pulse relationship and assess its impact on the accurate input-output pulse relationship. The input-output pulse relationship on the right side may be impacted by noise and chirp effects in the system in several ways such as pulse distortion: The noise and chirp together can deform pulses, changing their duration and shape. While chirps can induce frequency-dependent changes in the pulse envelope, noise

can result in random oscillations. When compared to the input pulses, these effects may result in distorted or widened output pulses. In addition to the Chirp-induced frequency shift: When comparing the output pulses to the input pulses, there may be a frequency shift brought on by the chirp effect. The chirp's frequency-dependent fluctuation in the pulse envelope is what causes this shift. As a result, there may be a difference between the input and output pulses' centers of frequency. The impact of noise and chirp effects on the input-output pulse relationship might be more noticeable at greater input power levels. Pulse abnormalities may get worse.

In Figure (7), we focused on studying the effect of noise on the output of two types of pulses: Gaussian pulse and super-Gaussian pulse. The left side of the graph (“a”) represents the Gaussian pulse, while the right side (“b”) corresponds to the super-Gaussian pulse.

A Gaussian pulse has a bell-shaped waveform, while a super-Gaussian pulse is a more complex waveform containing additional waves. Both pulses had the same pulse width, specifically 1ps. By analyzing the results shown in Figure (7(“2b”)), we observed a decrease in the pulse width of the super-Gaussian pulse. This decrease is due to a phenomenon called negative feedback resulting from stimulated emission (stimulated emission refers to a process in which

photons stimulate the emission of additional photons in the material, amplifying the optical signal). In this case, the carrier density, which represents the number of charge carriers in the material, was modified by stimulated emission.

The negative feedback mechanism generated by stimulated emission plays a crucial role in regulating the carrier density. As a result, it tends to suppress fluctuations in pulse amplitude, ultimately resulting in a narrower pulse width.

Overall, the study showed that the presence of additional waves in the ultra-Gaussian pulse, combined with the negative feedback effect of stimulated emission, contributed to a more stable and narrower pulse compared to the Gaussian pulse.

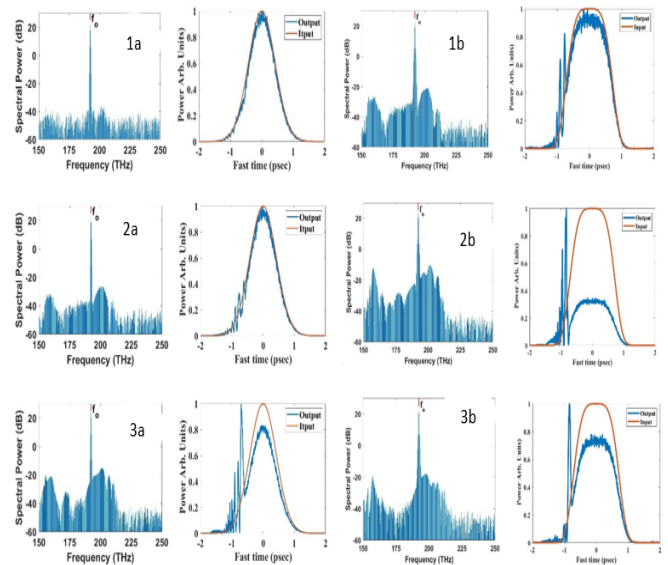


Fig. (7): OFC generated (left), input-output pulse relation (right) Gaussian pulse with noise (a) compared to super-

Gaussian pulse with noise (b), for input power is (1, 1.2, 1.5) W respectively.

4. Conclusion

We utilized a computational procedure, viz., the Lugiato-Lefever equation (LLE). A term was added to the LLE to include the noise effect on the microresonator dynamic. We used this term to control the levels of noise in our simulations to observe its impact on the formation and behavior of solitons and OFCs generated. It is noticed that noise affects the stability of the microresonator. The noise-optical input power relation showed that the noise effect was proportional to the input power. In conclusion, to reduce the noise effect on the microresonator, it must be run with an input of lower power, TEM₀₀ Gaussian mode. The study also examined the effect of noise, chirp, Gaussian, and super-Gaussian on the output of the microresonator. The study showed that there is a difference between the frequency centers of the input and output pulses. The effect of noise and chirp effects on the input-output pulse relationship may be more pronounced at larger input power levels. pulse disturbances may worsen.

References

[1] Herr, T., Hartinger, K., Riemensberger, J., Wang, C. Y., Gavartin, E., Holzwarth, R., Gorodetsky, M. L., and Kippenberg, T. J., 2012,

Universal formation dynamics and noise of Kerr-frequency combs in microresonators, *Nature Photonics* 6, 480-487,

[2] Herr, T., Riemensberger, J., Wang, C., Hartinger, K., Gavartin, E., Holzwarth, R., Gorodetsky, M. L., and Kippenberg, T. J., 2011, *Universal Dynamics of Kerr Frequency Comb Formation in Microresonators*, physics optics, 3071v1.

[3] Stern, B., Ji, X., Okawachi, Y., Gaeta, A. L., and Lipson, M., 2018, *Nature (London)*, 562, 401.

[4] Xiang, C., Liu, J., Guo, J., Chang, L., Wang R., Weng, W., Peters, J., Xie, W., Zhang, Z., Riemensberger, J., Selvidge, J., Kippenberg, J., and E. John Bowers, 2021, *Laser soliton microcombs heterogeneously integrated on silicon*, physics, optics, 373 (6550), 99-103

[5] Herr, T., Brasch, V., Jost, J. D., Wang, C. Y., Kondratiev, N. M., Gorodetsky, M. L., and Kippenberg, T. J., 2014, *Temporal solitons in optical microresonators*, *Nat. Photonics* 8, 145,

[6] Kippenberg, T. J., Gaeta, A. L., Lipson, M., and Gorodetsky, M. L., 2018, *Dissipative Kerr solitons in optical microresonators*, *Science* 361, ean8083

[7] Jasima, M. S., Sultan, H. A., and Emshary C. A., 2019, *The effect of attenuation and dispersion on the propagation of a short Gaussian pulse in optical fibers*, *Researcher*;11(1)

- [8] Abdul-Hussain Z. S., and Sultan, H. A. 2019, A theoretical study of soliton in photonic crystal fibers, *Researcher*, 11(1).
- [9] Maatoq, S., and Sultan, H. A., 2021, Optical frequency comb generation in semiconductor laser q switching and mode-locking, *IJASER*, 2(4).
- [10] Lucas, E, Karpov, M., Guo, H., Gorodetsky, M. L., and Kippenberg, T. J., 2017, Breathing dissipative solitons in optical microresonators, *Nat. Commun.* 8, 736
- [11] Karpov, M., Pfeiffer, M. H. P., Guo, H., Weng, W., Liu, J., and Kippenberg, T. J., 2019, Dynamics of soliton crystals in optical microresonators, *Nat. Phys.* 15, 1071
- [12] Qi-F. Yang, Yi, X., Yang, K. Y., and Vahala, K., 2017, Stokes solitons in optical microcavities, *Nat. Phys.* 13, 53
- [13] Bruch, A., Liu, X., Gong, Z., Surya, B., Li M., Zou, C., and Tang, X., 2021, Pockels Soliton Microcomb, *Nat. Photonics* 15, 21.
- [14] Bao, H., Cooper, A., Rowley, M., Lauro, L., Gongora, J., Chu, T., Little, E., Oppo, G., Morandotti, R., Moss, J., Wetzel, B., Peccianti M., and Pasquazi, A., 2019, Laser Cavity-Soliton Micro-Combs, *Nat. Photonics* 13, 384.
- [15] Nazemosadat, E., Fulop, A., Helgason O.B., Wang, P.-H., Xuan, Y., Leaird D. E., Qi, M., Silvestre, E., Weiner A. M., and Victor Torres-Company, 2021, Switching dynamics of dark-pulse Kerr frequency comb states in optical microresonators, *Phys. Rev. A* 103, 013513
- [16] Spencer, D. T., Drake, T., C. Briles, J. Stone, C. Sinclair, C. Fredrick, Q. Li, D. Westly, B. Robert Ilic, A. Bluestone, N. Volet, T. Komljenovic, L. Chang, S. Lee, D. Yoon Oh, M. Suh, K. Yang, H. P. Pfeiffer, T J. Kippenberg, E. Norberg, L. Theogarajan, R. Newbury, K. Srinivasan, E. Bowers, A. Diddams and Papp, B., 2018, An Integrated-Photonics Optical-Frequency Synthesizer, *Nature (London)* 557, 81
- [17] Obrzud, E., Rainer, M., A. Harutyunyan, M.H. Anderson, M. Geiselmann, B. Chazelas, S. Kundermann, S.Lecomte, M. Cecconi, A. Ghedina, E. Molinari, F. Pepe, F. Wildi, F. Bouchy, T.J. Kippenberg and Herr, T., 2019, A Microphotonic Astrocomb, *Nat. Photonics* 13, 31
- [18] Palomo, P., Kemal, N., Karpov, M., Kordts, A., J. Pfeifle, H. P. Pfeiffer, P. Trocha, S. Wolf, V. Brasch, H. Anderson, R. Rosenberger, K. Vijayan, W. Freude, T. J. Kippenberg, C. Koos, P.M., 2017, Microresonator solitons for massively parallel coherent optical communications *Nature (London)* 546, 274
- [19] West, N., Loh, W., Kharas, D., and Ram, J., 2020, Impact of laser frequency noise on high-extinction optical modulation, *Optics Express.* 28 (26).

- [20] Ahmed, M. F., 2003, Numerical characterization of intensity and frequency fluctuations associated with mode hopping and single-mode jittering in semiconductor lasers, ResearchGate.
- [21] Yang, Q., Ji, Q., L. Wu, B. Shen, H. Wang, C. Bao, Z. Yuan & Vahala, K., 2021, Dispersive-wave induced noise limits in miniature soliton microwave sources, *Nature Communications*.
- [22] Drake, T., Stone, J., Briles, T., & Pap, S., 2019, Thermal decoherence and laser cooling of Kerr microresonator solitons, *physics.optics*
- [23] Anashkina, A., Marisova, P., A. Sorokin and Andrianov, V., 2019, Numerical Simulation of Mid-Infrared Optical Frequency Comb Generation in Chalcogenide As_2S_3 Microbubble Resonators, *Photonics*.
- [24] Spencer, D. T., Drake, T., C. Briles, J. Stone, C. Sinclair, C. Fredrick Qing Li, D. Westly, B. Robert Ilic, A. Bluestone, N. Volet, T. Komljenovic, L. Chang, S. Hoon Lee, D. Yoon, M. Suh, K. Yang, P. Pfeiffer, T. J. Kippenberg, E. Norberg, L. Theogarajan, K. Vahala, R. Newbury, K. Srinivasan, E. Bowers, A. Diddams, Papp, S. B., 2018, An Integrated-Photonics Optical-Frequency Synthesizer, *Nature (London)* 557, 81.
- [25] Coen, S., Randle, H. G., Sylvestre, T., and Erkintalo, M., 2013, Modeling of octave-spanning Kerr frequency combs using a generalized mean-field Lugiato-Lefever model, *Opt. Lett.* 38, 37-39
- [26] Xue, X., Xuan, Y., Liu, Y., Wang, PH., S. Chen, J. Wang, D. ELeaird, M. Qi, Weiner, A., 2015, Mode-locked dark pulse Kerr combs in normal-dispersion microresonators. *Nature Photonics* 9:594–600. 10.1038/nphoton.13.
- [27] Sumetsky, M., 2023, Semiclassical theory of frequency combs generated by parametric modulation of optical microresonators, Aston Institute of Photonics Technologies, Aston University, Birmingham B4 7ET, UK,
- [28] Seibold, K., Rota, R., Minganti, F., and Savona, V., 2021, Quantum dynamics of Dissipative Kerr solitons, *quant-ph*, December.
- [29] Agrawal, G., 2006, *Nonlinear Fiber Optics*, Academic, San Diego.
- [30] Hansson, T., Wabnitz, S., 2015, Frequency comb generation beyond the Lugiato–Lefever equation: multi-stability and super cavity solitons. *Journal of the Optical Society of America B*, 32(7),1259–1266, 10.1364/JOSAB.32.001259.
- [31] Brasch, V., Geiselmann, M., Herr, T., Lihachev, G., Pfei_er, M. H. P., M., Gorodetsky, L., and Kippenberg, T. J., 2016, Photonic chip-based optical frequency comb using soliton Cherenkov radiation, *Science*, 351, 357
- [32] Ji, X., Barbosa, F. A. S., Roberts, S. P., Dutt, A., Cardenas, J., Okawachi, Y., Bryant, A., Gaeta, A. L., and Lipson, M., 2017, Ultra-low-

loss on-chip resonators with sub-milliwatt parametric oscillation threshold, *Optica*, 4, 619

[33] Zhang, X., Luo, H., Xiong, W., Chen, X., Han, X., Xiao, G., and Feng, H., 2021, Numerical investigation of turnkey soliton generation in an organically coated microresonator, *Phys. Rev. A* 103, 023515, Published 12 February.

[34] Herr T., Hartinger, K., Riemensberger, J., Wang, C. Y., Gavartin, E., Holzwarth, R., Gorodetsky, M. L., and Kippenberg, T. J., 2012, Universal formation dynamics and noise of Kerr-frequency combs in microresonators. *Nature Photonics* 6, 480-487.

[35] Murakawa, T., Konishi, T., 2015, Pulse-by-pulse near 800-nm band power stabilization using all-optical limiter based on self-phase modulation. *Optics Communications*, 344, 134-138

[36] Pan J., Xu, C., Wu, Z., Zhang, J., Huang, T., Shum, P. P., 2022, Dynamics of cavity soliton driven by chirped optical pulses in Kerr resonators, *Frontiers of Optoelectronics*.